Phase/Amplitude Synchronization of Brain Signals During Motor Imagery BCI Tasks

Tiziana Cattai, Stefania Colonnese, *Senior Member, IEEE*, Marie-Constance Corsi, Danielle S. Bassett, Gaetano Scarano, and Fabrizio De Vico Fallani

***Abstract*— In the last decade, functional connectivity (FC) has been increasingly adopted based on its ability to capture statistical dependencies between multivariate brain signals. However, the role of FC in the context of brain-computer interface applications is still poorly understood. To address this gap in knowledge, we considered a group of 20 healthy subjects during an EEG-based hand motor imagery (MI) task. We studied two well-established FC estimators, i.e. spectral- and imaginary-coherence, and we investigated how they were modulated by the MI task. We characterized the resulting FC networks by extracting the strength of connectivity of each EEG sensor and we compared the discriminant power with respect to standard power spectrum features. At the group level, results showed that while spectral-coherence based network features were increasing in the sensorimotor areas, those based on imaginary-coherence were significantly decreasing. We demonstrated that this opposite, but complementary, behavior was respectively determined by the increase in amplitude and phase synchronization between the brain signals. At the individual level, we eventually assessed the potential of these network connectivity features in a simple off-line classification scenario. Taken together, our results provide fresh insights into the oscillatory mechanisms subserving brain network changes during MI and offer new perspectives to improve BCI performance.**

***Index Terms*— EEG, functional connectivity, network theory, brain-computer interface.**

Manuscript received December 7, 2020; revised March 12, 2021; accepted March 28, 2021. Date of publication June 11, 2021; date of current version June 28, 2021. This work was supported by the Investissements d'avenir Program (Agence Nationale de la Recherche-10-IA Institut Hospitalo-Universitaire-6) under Grant ANR-10-IAIHU-06. The work of Fabrizio De Vico Fallani was supported in part by the Agence Nationale de la Recherche through under Contract ANR15-NEUC-0006-02 and in part by the European Research Council (ERC) under the European Union's Horizon 2020 Research and Innovation Programme under Grant 864729. *(Corresponding author: Fabrizio De Vico Fallani.)*

This work involved human subjects or animals in its research. Approval of all ethical and experimental procedures and protocols was granted by the Ethical Committee CPP-IDF-VI of Paris.

Tiziana Cattai is with Inria Paris, Aramis Project Team, 75012 Paris, France, also with the Institut du Cerveau, ICM, 75013 Paris, France, also with the Inserm, U 1127, 75013 Paris, France, also with CNRS, UMR 7225, Sorbonne Universite, 75013 Paris, France, and also with the Department of Information Engineering, Electronics and Telecommunication, Sapienza University of Rome, 00184 Rome, Italy.

Stefania Colonnese and Gaetano Scarano are with the Department of Information Engineering, Electronics and Telecommunication, Sapienza University of Rome, 00184 Rome, Italy.

Marie-Constance Corsi and Fabrizio De Vico Fallani are with Inria Paris, Aramis Project Team, Paris, France, and also with the Institut du Cerveau, ICM, Inserm U 1127, CNRS UMR 7225, Sorbonne Universite, 75013 Paris, France (e-mail: fabrizio.devicofallani@gmail.com).

Danielle S. Bassett is with the Department of Bioengineering, the Department of Electrical and Systems Engineering, and the Department of Physics and Astronomy, University of Pennsylvania, Philadelphia, PA 19104 USA, and also with the Department of Neurology and the Department of Psychiatry, Hospital of the University of Pennsylvania, Philadelphia, PA 19104 USA.

This article has supplementary downloadable material available at https://doi.org/10.1109/TNSRE.2021.3088637.

Digital Object Identifier 10.1109/TNSRE.2021.3088637

I. Introduction

BASED on the classification of mental states from brain signals, brain-computer interfaces (BCIs) are increasingly explored for control and communication, as well as for the treatment of neurological disorders (e.g. stroke), particularly via the ability of subjects to voluntary modulate their brain activity through mental imagery. The ability to correctly detect the user's mental intent is therefore a crucial factor in the design of BCI systems [1]–[6].

To this end, researchers have explored in the last decade several approaches based on disparate theoretical and experimental grounds. On one hand, investigators have focused on the identification of the best mental strategy to detect the user's intent or on the choice of the sensory feedback to convey the most relevant information to the user [7]–[9]. On the other hand, advanced signal processing methods and sophisticated classification algorithms have been developed to improve the signal-to-noise ratio and to correctly identify the user's intent [10]. While these methods can provide considerable performance increments, they are intrinsically blind to the neural mechanisms that allowed investigators to classify the user's intent and may not have an obvious physical or physiological interpretation [11]. However, this is crucial especially in clinical settings where brain functioning can be compromised and alternative solutions must be identified.

An alternative approach would consist in looking for different - potentially more informative - features characterizing the human brain functional organization. To this end, functional connectivity (FC) has been introduced to estimate the interaction between spatially distributed brain areas by measuring the temporal dependence between the regional activities [12]. Thus, in contrast to univariate features such as frequency band power, FC appears more appropriate to capture the oscillatory network mechanisms involved in brain (re)organization during mental tasks [13]. Recent results have demonstrated the potential of FC features in BCI [14]–[16], albeit the results are variable and difficult to compare because of the different FC estimators, tasks and limited number of

This work is licensed under a Creative Commons Attribution 4.0 License. For more information, see https://creativecommons.org/licenses/by/4.0/

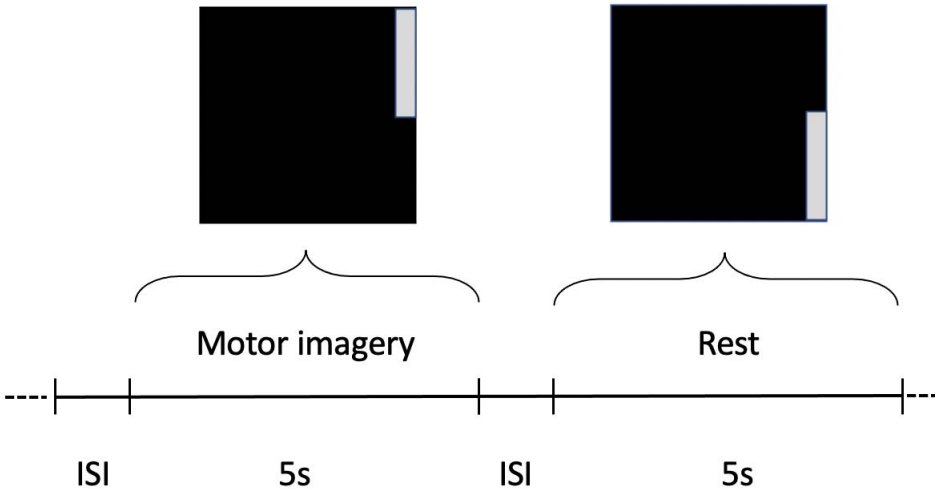

Fig. 1. Time course associated with BCI protocol. The BCI experiment consisted in a standard 1D, two-target box task. When the target was up, the subject was instructed to perform a right hand motor imagery (i.e. grasping); when the target was down, the subject had to remain at rest. In each trial, the first second corresponded to the inter-stimulus interval (ISI), when a black screen was presented to the subject. During the following 5s, the target appeared on the screen and during this period subjects had to imagine a sustained grasping of their right dominant hand.

subjects used in those studies [17]–[20]. More importantly, the neurophysiological and mechanistic interpretation of FC features is still poorly understood in motor imagery tasks but this is critical to eventually design alternative FC-based BCIs.

To address this question we considered two well-established FC estimators, i.e. the spectral-coherence and imaginary-coherence [21], [22]. From a theoretical perspective, these estimators bring complementary information since the first measures the synchronization between the signal amplitudes while the latter is also sensitive to their phase difference [22], [23]. We hypothesized that integrating these complementary features will allow a better characterization of the BCI-related mental states and that including them in the feature extraction block would serve to increase the BCI accuracy as compared to standard approaches solely based on power spectra. To test these predictions, we considered brain FC networks derived from EEG data recorded in a group of 20 healthy subjects performing the motor imagery (MI) of the right hand grasping. To allow a fair comparison with the results obtained with power spectrum features, we extracted for each sensor the node strength, an intuitive graph theoretic metric quantifying its overall connection intensity within the network. At the group level, we compared the spatial patterns extracted by statistically contrasting the feature values in the MI with respect to a baseline condition, where subjects were at rest. At the individual level, we evaluated the associated performance by means of an *off-line* classification simulation.

II. Material and Methods

A. Experimental Protocol and Preprocessing

Twenty healthy subjects, all right-handed, were included in the study. All subjects were BCI naive and they were recruited within the framework of a BCI training protocol. They did not present with any medical or psychological disorder. The study was approved by the ethical committee CPP-IDF-VI of Paris and each subject signed an informed consent. All participants received financial compensation for their participation. EEG data were recorded with a 74-channel system, with Ag/AgCl sensors (Easycap, Germany) in a 10-10 standard configuration. The reference for the EEG signals were mastoid signals and the ground electrode was on the left scapula. Data were recorded in a shielded dimly lit room. Impedances were kept lower than 20 kOhms; the sampling frequency was set to 250 Hz. During the experiments, hand muscular activity was recorded with EMG (electromyogram) to check the presence of involuntary movements during the motor imagery tasks. On-line, the experimenter ensured that subjects were not generating muscular artifacts during the task. Off-line, all the recorded signals have been checked to exclude the presence of evident muscular artefacts. The BCI experiment consisted in a standard 1D, two-target box task [24]. The subject was in front of a screen with a distance of 90 cm. When the target was up, the subject was instructed to imagine moving his/her right hand (i.e. grasping); when the target was down, the subject had to remain at rest. For each subject we collected 64 trials of motor imagery and 64 trials of resting state. In each trial, the first second corresponded to the inter-stimulus interval (ISI $\sim$ 1s), when a black screen was presented to the subject. For the following 5s the target appeared on the screen; in this period subjects had to imagine a sustained grasping of their right dominant hand. We report in Fig.1 a graphical representation of the time-line for a typical trial. We refer to [25] for a detailed description of the experiments.

As a pre-processing we performed on the entire dataset an independent component analysis (ICA) to eliminate ocular and cardiac artifacts on the EEG signals, via the Infomax algorithm [26] available in the Fieldtrip toolbox [27]. The ICA was operated by the visual inspection of both time signals and their associated topographies. We removed no more than two independent components.

In order to measure the ability of connectivity features to characterize other motor imagery tasks, we also used the EEG

data from dataset 1 of BCI competition IV [28]. EEG data were recorded from 59 electrodes, which enabled us to obtain a number of nodes similar to our data. From this dataset we considered 4 healthy subjects each one performing different MI tasks (left/ foot for subject a; left/ right for subject b; left, foot for subject f and left, right for subject g).

B. Functional Connectivity and Brain Network Features

We considered two well-established functional connectivity estimators [29], i.e. spectral coherence (C) [21] and imaginary coherence (IC) [22]. While other FC estimators, directed and undirected, have been previously explored in the BCI context [17], [30]–[33], here we focused on C and IC because of their relatively simplicity and intuitiveness.

Given two EEG time series x_j and x_k in a time interval T, the computation of C_{jk} and IC_{jk} at the frequency f can be respectively obtained as:

$$C_{jk}[f] = \frac{|P_{jk}[f]|}{\left(P_j[f] \cdot P_k[f]\right)^{1/2}} \tag{1}$$

$$IC_{jk}[f] = \frac{|\Im\left(P_{jk}[f]\right)|}{\left(P_j[f] \cdot P_k[f]\right)^{1/2}} \tag{2}$$

where $P_j[f]$ contains the samples of the power spectral density $P_{jj}(e^{i\omega})$ estimated on T-length windows, i.e. $P_j[f] = P_{jj}[f](e^{i\omega})|_{\omega=\omega_f}$, with the angular frequency $\omega_f = 2\pi f/T$; and $P_{jk}[f]$ are samples of the cross-spectrum $P_{jk}(e^{i\omega})$ between x_j and x_k.

These quantities are evaluated by means of with Welch's method with Hanning time windows of $T = 1\ s$ and an overlap of 50% [34]. While C has an intuitite interpretation the advantage of capturing linear correlations in the frequency domain, IC, by neglecting zero-lag contributions, is more robust to spurious connectivity due to volume condition [22]. For this reason, coherence is more sensitive to short-range interactions while imaginary coherence is weights more long-distance connections [35]. To directly quantify the phase relationship between two EEG signals at the frequency f, we computed their phase difference Δ:

$$\Delta_{jk}[f] = |\phi_j[f] - \phi_k[f]| \tag{3}$$

where $\phi_j[f]$, $\phi_k[f]$ are the phase terms of the discrete Fourier transforms (DFTs) of x_j and x_k on T-samples windows.

By computing C, IC and Δ for each pair of EEG channel, we obtained symmetric $N \times N$ matrices where $N = 74$ is the number of EEG channels. These matrices correspond to fully connected and weighted networks of N nodes or units and can be studied via graph theoretic tools [12]. Here, we focused on a simple local centrality measure, i.e. the node strength S, which is given by the sum of the weights of all links coming into each node. This metric describes in an intuitive way how much one brain region, or EEG channel, is connected to all the others in a certain frequency f. Hence, node strengths were computed for each connectivity estimator used to extract the network, as follows :

$$S_j^C[f] = \sum_{k=1}^{N} C_{jk}[f], \tag{4}$$

$$S_j^{IC}[f] = \sum_{k=1}^{N} IC_{jk}[f], \tag{5}$$

$$S_j^{\Delta}[f] = \sum_{k=1}^{N} \Delta_{jk}[f] \tag{6}$$

C. Statistical Analysis and Classification

At group level, we averaged for each subject the corresponding connectivity matrices across trials and within predefined frequency bands, commonly involved in motor imagery tasks [36], namely: $theta = 4 - 7$Hz, $alpha = 8 - 13$Hz, $beta = 14 - 29$Hz and $gamma = 30 - 40$Hz. Node strengths were extracted from each of these resulting networks. The same procedure was adopted for power spectrum-based features.

We statistically compared connectivity and node strength values between MI and Rest conditions. More specifically, for each condition we considered the distributions of the values obtained from the entire population of 20 subjects. We used permutation t-tests (2000 permutations) with a statistical threshold of 0.05 [37].

At individual level, we kept the original information and we did not average the results across trials or within frequency ranges. We let the classification procedure to optimally select the best discriminant features for MI and Rest conditions. We only imposed some constraints to limit the research complexity. First, we considered frequency bins from 4 to 40 Hz, due to prior reports supporting their involvement in similar motor tasks [38]. Second, we limited the research among a subset of electrods spatially covering the sensorimotor areas [39].

With the aim of comparing the contribution of the three different type of features to the overall classification we considered all their possible combinations, i.e. seven in total. To normalize the values in each combination, we applied a z-score transformation to original features, i.e. channels $\times$ frequency bins. Then, we performed a 100 repeated ten-fold cross-validation test with linear discriminant analysis (LDA) [10]. Specifically, we performed a sequential feature selection [40] within a nested cross-validation framework. Specifically, at each cross-validation step, we sorted in a descending order the available features from the training folds according to their t-values. All statistical results were corrected for multiple comparisons with false discovery rate (FDR) [41].

III. Results

A. EEG Network Connectivity Changes During Motor Imagery

We first verified that subjects were performing a proper motor imagery task by showing sensorimotor power decreases mainly in frequency bins within *alpha* and, more pronouncedly, *beta* band ($p < 0.05$, FDR-corrected) (**Fig. S1**). Network connectivity changes between MI and Rest conditions could be appreciated across all the frequency bands (**Fig. S2** and **S3**). In the *beta* band, results tended to occur in motor-related areas contralateral to the imagined movement.

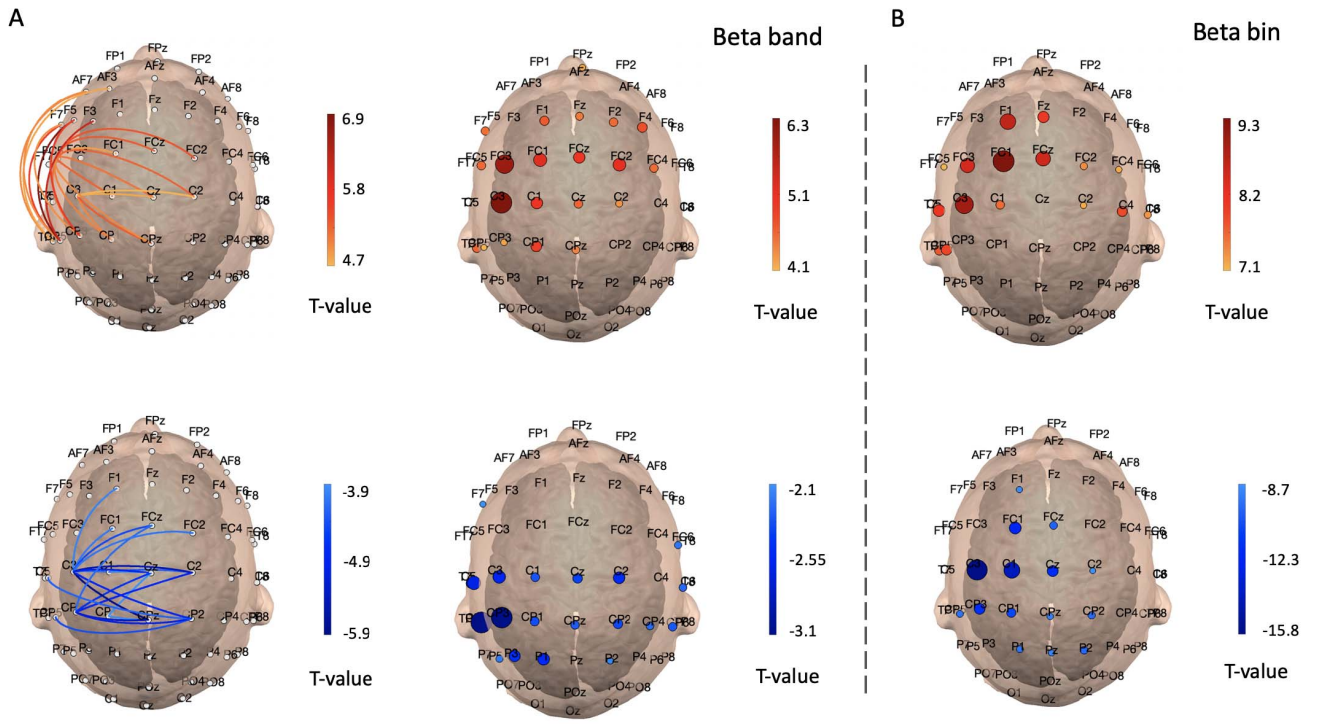

Fig. 2. Statistical contrast maps between motor imagery and resting states in the *beta* band. In panel A, we report the results in *beta* band for connectivity and node strength values. In panel B, we show the results of node strength for individual representative frequency bins within the *beta* band. Results for coherence-based features are in top line, while those for imagery coherence-based features are in bottom line. Only the twenty most discriminant values are represented here for illustrative purposes.

This could be observed both for single connection and node strength values (Fig. 2A). These changes were even stronger when considering node strength values at individual frequency bins ($p < 0.05$, FDR-corrected) (Fig. 2B).

Notably, the direction of the change is opposite depending on whether we used spectral-coherence (C) or imaginary-coherence (IC) to estimate EEG networks. We reported significant MI-related increases when we considered C estimators, while we observed significant decrements when using IC. In terms of spatial locations these differences involved both intra-hemispheric and inter-hemispheric interactions, while the largest changes in node strength tended to concentrate around the brain areas corresponding to the EEG electrode $C3$.

We observed a similar behavior for *gamma* frequency band, although the most involved regions were more heterogeneously distributed. On the contrary, we could not find similar trends for *theta* and *alpha* bands, where modifications were in the same direction (**Fig. S2** and **Fig. S3**).

In general, the magnitude of network changes was larger compared to power P features (Fig. 2B, **Fig. S1**). Furthermore, the results obtained with node strength were not associated with those obtained by using P values (Pearson's correlation < 0.1).

These findings indicated that the motor imagery of the hand grasping elicits detectable brain network changes that might be useful to characterize and discriminate MI-based BCI tasks. These changes revealed the existence of two parallel connectivity behaviors (i.e. increase for C and decrease for IC) that primarily involved sensorimotor areas within *beta* frequencies.

B. Modulation of Amplitude and Phase Synchronization Between Brain Signals

To better understand the nature of such dichotomy, we investigated more in detail the behavior of C and IC estimators. C is obtained from the cross-spectrum of the two signals and is sensitive to the amplitude synchronization (AS), i.e. when signals oscillate (or vary) at the same frequency. IC is also sensitive to the phase synchronization (PS) capturing possible time shifts between the signals.

To show these behaviors, we considered two perfectly equal sine waves oscillating at 10 Hz, and we temporally shifted one with respect to the other within the $[-\pi/2, \pi/2]$ interval. Fig. 3A,B shows that C remains constant along the entire phase shift range, while IC varies in a way that it tends to zero when the two signals are perfectly in phase (i.e. $\Delta = 0$). In a supplemental analysis, we indeed demonstrated that the imaginary coherence between those signals can be analytically expressed as a function of their relative time delay (**Supplementary text**).

Our experimental results showed that during MI there is a simultaneous amplitude synchronization (captured by C) and phase-synchronization (captured by IC), the latter suggesting a significant signal phase alignment (Fig. 2). To confirm this finding, we re-estimated the task-related brain networks by computing the phase difference Δ between the EEG signals.

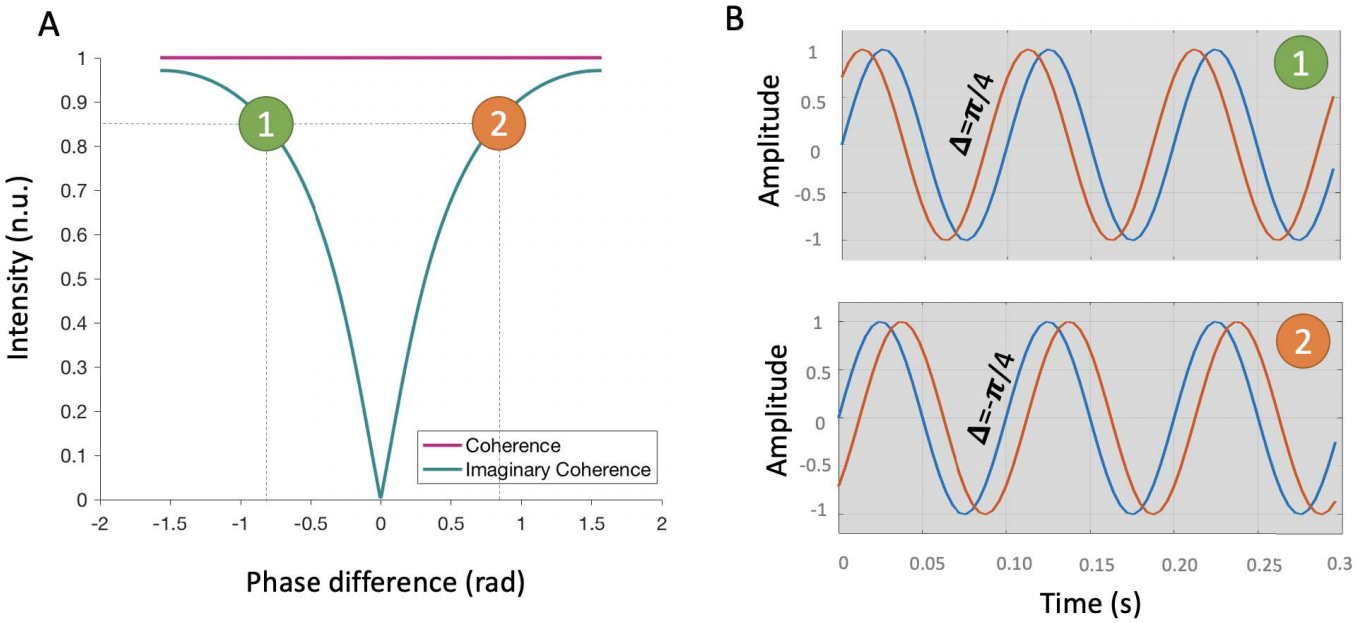

Fig. 3. Relationships of coherence/imaginary coherence with phase difference. In Panel A) coherence is in pink and imaginary coherence in green, showing the functional connectivity between two sine waves at 10 Hz as function of their temporal shift. The shift, corresponding here to a phase difference, varies from 0 to π in steps of π /500. At each shift value, the two connectivity estimators are evaluated. Panel B) shows the sine waves with different phase differences. In panel 1), a positive Δ of π /4 in panel 2), a negative Δ of $-\pi/4$.

For both single connection and node strength statistics we reported a global significant decrease which is actually similar, in terms of magnitude and spatial arrangement, to what observed with IC (**Fig. 4**A,B).

More formally, we investigated the MI task-related relationship between imaginary coherence and relative phase difference. For each subject, we considered all the pairs of nodes including the $C3$ sensor, representing the contralateral primary motor area of the hand. Results showed a moderate correlation (group-median Spearman's $R = 0.38$) with lower Δ values predicting lower IC values (**Fig. 4C**, **Table S1**).

These findings indicated that hand MI elicits a two-fold mechanism supporting more efficient information transfer - in terms of AS and PS - among sensorimotor brain regions.

C. Mental State Detection in Single Individuals

Finally, we tested the ability of these brain connectivity features to discriminate MI and resting states at single subject level. To increase specificity, we considered a finer frequency resolution of 1 Hz - from 4 to 40 Hz - and we restricted the feature extraction to the EEG electrodes in the sensorimotor areas (see Materials and Methods).

For each MI and rest trial we extracted three type of features: power spectrum P, coherence-based node strength S^C and imaginary coherence-based node strength S^{IC}. We checked that all the covariance matrices associated with the features verified that their overall sum were not statistically different between conditions (t-test, $p > 0.05$). To identify the best discriminant feature combination, we performed a sequential forward feature selection within a cross-validation linear discriminant analysis (LDA). We used the overall accuracy to measure the average classification performance across validations.

Results showed that the best classification accuracy was in general moderate regardless of the feature combination (**Table S2**). However, we observed that the inclusion of node strength features led to performance increment in terms of relative difference with respect to P features alone (**Fig. 5**). That was particularly evident when selecting features from the contralateral hemisphere (16 subjects over 20) as compared to when we considered both hemispheres (12/20). For contralateral areas, the performance increment corresponding to the best features combination was up to 25%.

We also reported a similar trend when using another EEG dataset from the BCI competition IV [28]. The inclusion of S^C features notably allowed to slightly increase classification accuracy in three over four subjects, ie 1%, 1.1%, and 2.5% in terms of relative increment (**Fig. S4**).

To identify the spatial and spectral characteristics of the selected features, we showed their cumulative occurrence in a frequency-sensor plot (**Fig. 6**). In general, we observed a concentration of features in the $10 - 14$ Hz range within the $C\text{-}CP$ zone. For both P and S^C, the occurrences at higher frequencies tended to fade out [**Fig. 6** (top and middle line)] while the situation was more heterogeneous for S^{IC} features [**Fig. 6** (bottom line)].

Finally, we performed a supplementary classification by substituting standard power spectrum features with those obtained with a more advanced method, namely the filter bank common spatial pattern (FBCSP) [42]. The obtained results showed that using FBCSP features was not significantly improving the overall accuracy and that node strength values still contributed to the relative performance improvement (**Table S3**, **Fig. S5**).

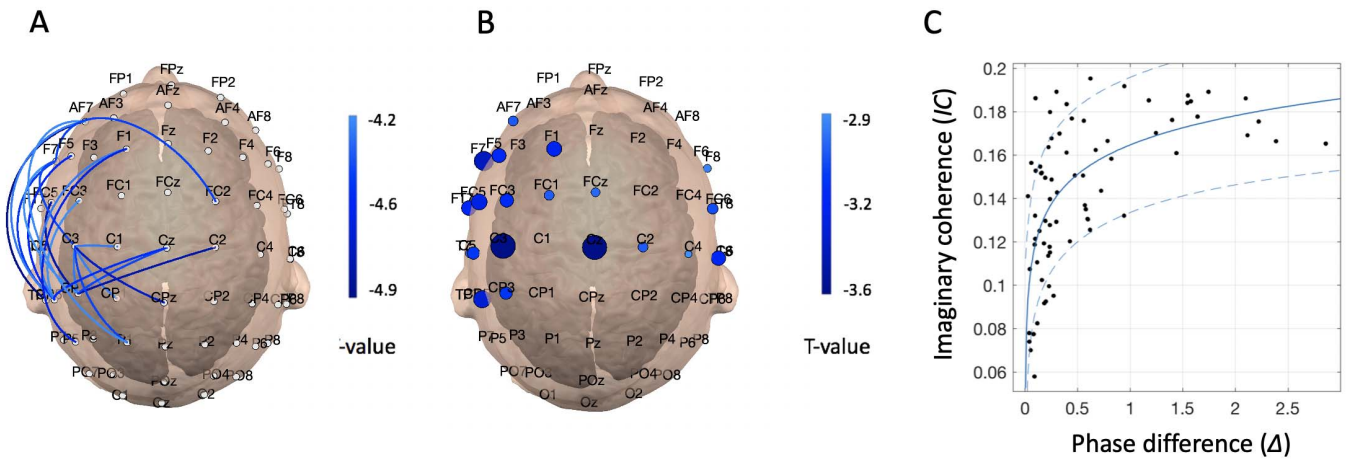

Fig. 4. Phase difference properties and discrimination ability. Panel A), results of permutation-based t-tests in the *beta* band across all subjects are shown for brain networks reconstructed from the phase difference between EEG signals. Panel B) results of permutation-based t-tests obtained with node strength values extracted from the previous brain networks. Panel C), Spearman correlation plot between imaginary coherence and phase difference values considering all the connections including C3 electrode for one representative subject.

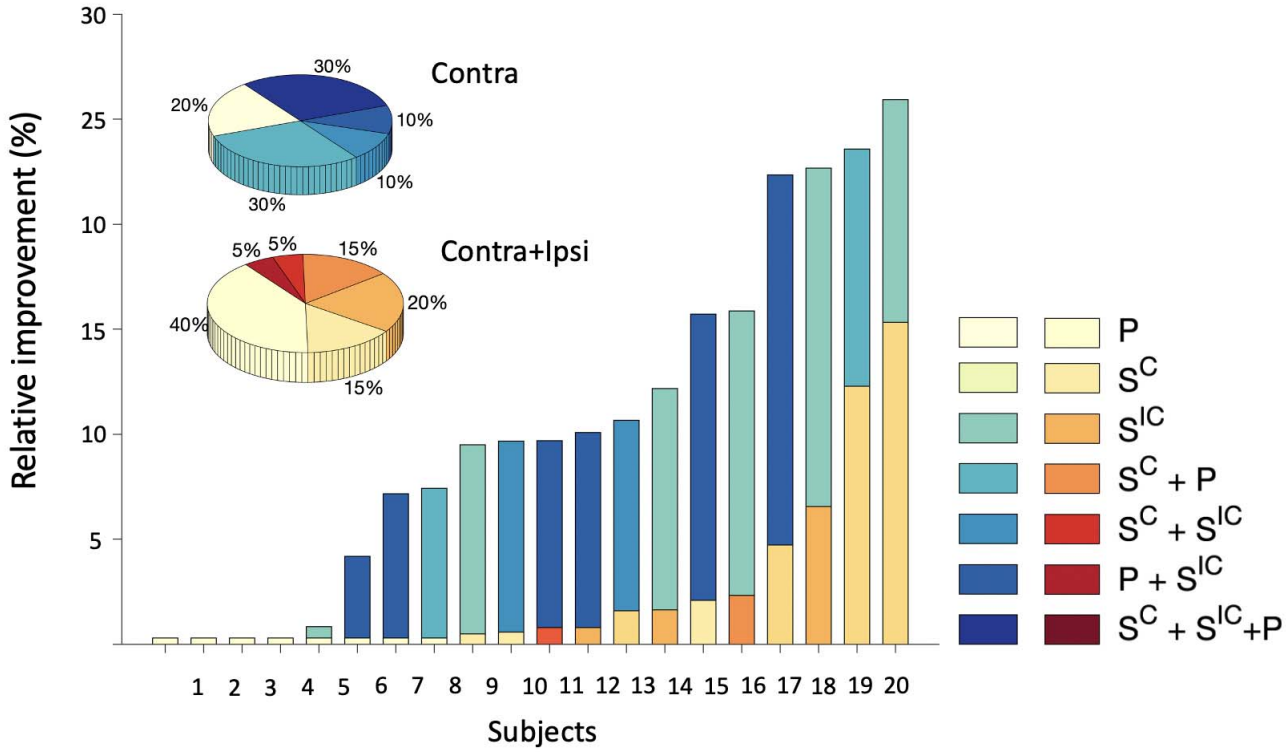

Fig. 5. Improvement of classification performance. Bar plots show the percentage of relative increment between the best combination of features (i.e., coherence-based node strength S^C, imaginary coherence-based node strength S^{IC} and power spectrum P. The pie diagram in the inset illustrates the percentage of times that a specific combination of features has been selected across subjects.Two different cases are considered, distinguished by a different color code. In blue, we report results of accuracy improvements when selected electrodes are located in contralateral sensorimotor area (Contra), ie. FC5, FC3, FC1, C5, C3, C1, CP5, CP3, CP1. In red, results relate to classification analysis when electrodes are in both contralateral and ipsilateral sensorimotor areas (Contra+Ipsi), ie. FC5, FC3, FC1, C5, C3, C1, CP5, CP3, CP1, FCZ, CZ, CPZ, FC2, FC4, FC6, C2, C4, C6, CP2, CP4, CP6.

Taken together, these results showed the potential of brain network features, derived from both amplitude and phase synchronization, to detect motor imagery states in healthy subjects.

IV. Discussion

Brain activity changes during motor tasks have been largely documented through invasive and noninvasive neuroimaging techniques in non-human and human primates, as well as in animal models [43]–[45]. These changes were not limited to specific brain areas, but also occur in a coherent and synchronized manner across larger spatial scales - from millimeters to centimeters - reflecting the need for a coherent coordination of information exchanges to accomplish the task [46]–[49]. Functional connectivity methods, estimating temporal dependence between spatially remote brain areas, represent therefore a

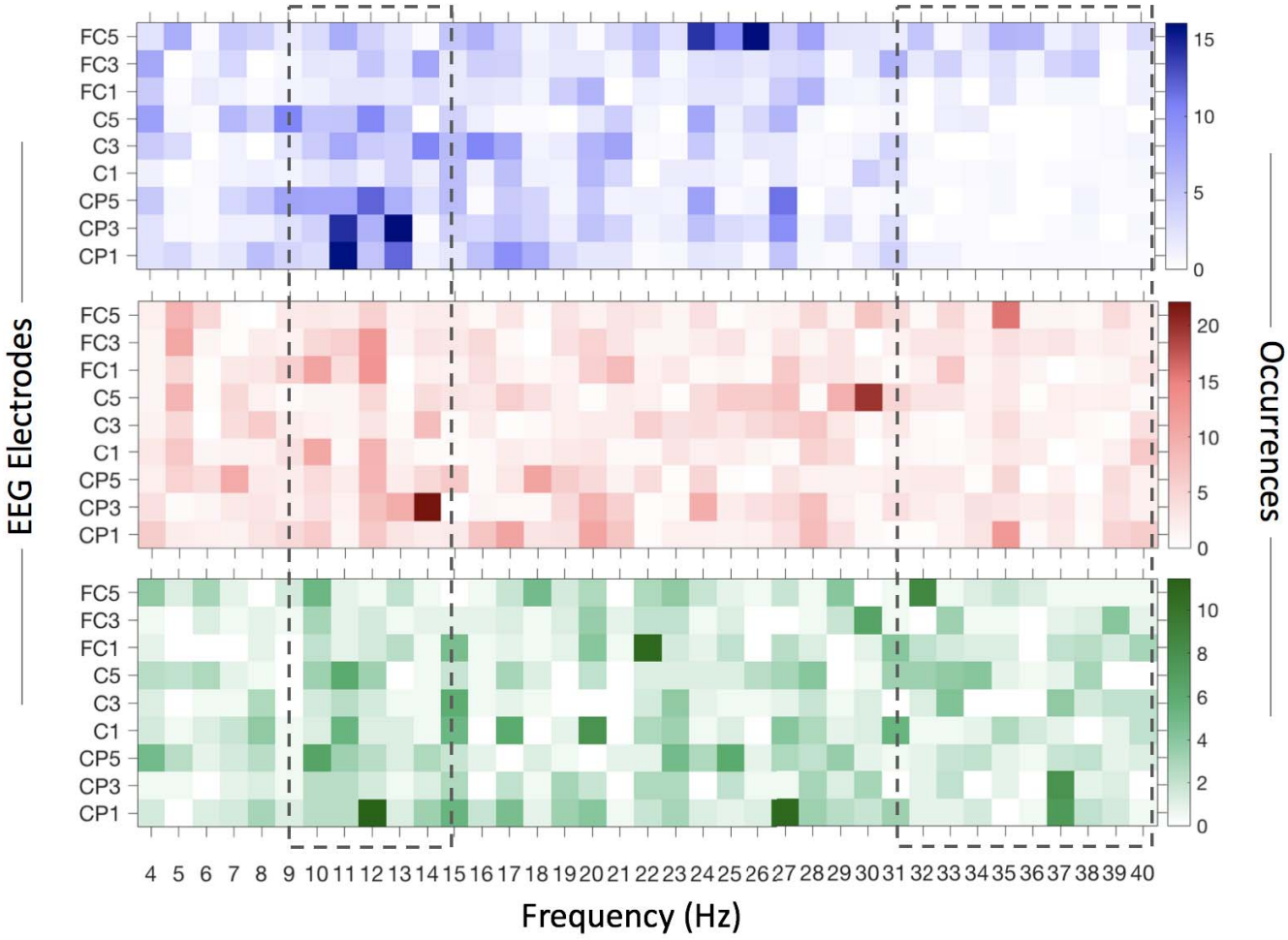

Fig. 6. Brain features selected by the classification procedure. The color codes for the group-averaged number of times that a specific feature - in the electrode-frequency space - has been chosen during the sequential feature selection algorithm. The results for P features are illustrated in the top line, those for S^C in the middle line and those for S^{IC} in the bottom line. Results relates to the classification analysis framework when only electrodes in the contralateral sensorimotor area are selected.

unique opportunity to study large-scale brain network changes during motor tasks from noninvasive EEG recordings.

In practice, many methods have been proposed to estimate FC based on different principles from signal processing and information theory [18], [31], [32], [50], [51].

Previous works reported FC modulations in both healthy and diseased subjects [52], [53], as well as in BCI contexts [17], [30]–[33]. However, different FC estimators have been used in those studies and a deeper understanding of the meaning of obtained FC values was in general overlooked. As a result, a common direction and principled interpretation of the changes observed during BCI motor-related tasks is still lacking [33].

To deepen this aspect, we investigated the intrinsic nature of two popular and intuitive FC estimators, spectral coherence and imaginary coherence, and realized a simple motor imagery task in a group of healthy subjects. Our results indicate that motor imagery elicits two major parallel oscillatory phenomena in the *beta* and *gamma* frequency bands: *i)* the increase of synchronization between the EEG signal amplitudes, *ii)* a decrease of phase difference, which means an increase of synchronization between signal phases. Both amplitude and phase synchronization increments have been respectively reported in separate studies. The former typically codes for a basic substrate of neural communication [54], while the latter occurs to further favor information binding [55]. These network connectivity changes were region-specific and more evident for the in the sensorimotor areas in the *beta* band, which is typically involved in motor-related tasks [36]. They particularly emerged at the node strength level (i.e. aggregating the information from all the nodal connections) and were not correlated with other regional measures, such as standard power spectral densities.

Taken together, these results unveiled the presence of a parallel amplitude and phase synchronization during MI at the higher frequency bands (i.e. *beta* and *gamma*). This complementary phenomenon was not observed in the lower bands (*theta* and *alpha*), where we rather found increased AS but decreased PS, as quantified by increased IC-based features. While this behaviour might appear counter-intuitive, it nevertheless matches with the complex spectrum of configurations that mechanistically emerge from the interactions of oscillatory signals [56]. In neuroscience applications, it has been actually shown that there could be phase-coupling without

amplitude-coupling and vice-versa [57]. More in general, our results show that MI elicits FC network changes across multiple frequencies. EEG coupling changes in *theta* and *alpha* bands have been previously found during sensorimotor integration tasks, such as mental navigation, and associated with deeper hippocampal *theta* oscillations [58], [59]. Modifications in higher frequency have been instead associated with direct motor-related demands and therefore proposed to be more robust for BCI applications [32]. Whether these latter high-frequency changes also include indirect effects due to mirror-neuron activity as well as attentional efforts associated with the task complexity, still remains to be elucidated [45].

The ability to discriminate different mental states from non-invasive neuroimaging recordings has concrete implications in our daily-life, from the early detection of brain diseases to the development of effective brain-computer interface applications [60]. In the BCI context, much of the efforts has focused on the improvement of the classification algorithms, such as the recent advances in Riemannian geometry-based approaches [61], [62]. While these methods can in some cases ameliorate the overall classification accuracy, the improvement potential is still high and, more importantly, they generally lack of intuitive physiological interpretations [10], [13]. The research of alternative features, beyond the characterization of single region activities, is therefore a fertile field with the aim of pursuing performance [18], [33], [51], [63]–[65].

Whether the use FC features, or network-based ones, brings significant BCI classification improvements, is still under debate [18], [30], [33], [51], [66], [67]. Our results indicated that node strength features bring complementary information with respect to power-spectrum features and hold the potential to improve classification accuracy. This might have concrete implications in the design of future BCI, where the features selection is typically performed in the calibration phase. However, it is important to state the performance increments obtained here significantly varied across individuals and led in general to moderate overall accuracy. While our contribution highlights the potential of brain network-based features in addressing BCI inefficiency issues, future studies will be crucial to assess the actual ability to discriminate between multiple mental states [68].

Spectral coherence and imaginary coherence assume the stationarity of time series within the period of interest [22]. In our study, we considered time windows 5 s, which could be too long for respecting this hypothesis [69]. We assessed the reliability of our results by computing the augmented Dickey-Fuller test [70] and verifying that 96% of all the signals were indeed stationary. More in general, for real-time BCI applications the use of shorter time windows and FC estimators that do not need stationarity assumptions (e.g. wavelets [71], tracking algorithms [72]), would naturally allow to circumvent this issue.

A. Methodological Considerations

Our analysis has focused on the EEG sensor space. Coherence-based FC estimators could be affected by volume conduction distortions introducing spurious signal interactions [22], [73]. While source-reconstruction techniques could be used to attenuate such bias [74], we decided to work on the sensor space for two main reasons. First, we did not have access to the individual magnetic resonance images (MRIs) necessary to have a detailed and realistic model of the head and its compartments [75]–[77]. Second, FC estimators can be really sensitive to signal transformations and results could be strongly dependent to the selected reconstruction algorithm [78]. A detailed analysis on the effects of source-reconstruction was, however, beyond the scope of our study. Further research is expected to better investigate the stability of our results when working at source space level.

When combining different types of brain characteristics (i.e. power, node strengths), we performed a fusion at the feature space level [79]. Another possibility would be to perform the fusion at the classifier level, by combining the posterior probabilities of each separate classification [25]. However, the latter approach will force the research of significant features in each modality despite their absolute discriminant power. To allow a fair comparison with band-power features, we preferred let the classifier identify the best absolute combination of features. We verified that the lengths of the selected feature vectors was in average similar (five features maximum).

V. Conclusion

The main purpose of our work consists in characterizing brain network connectivity changes during motor imagery-related BCI tasks. The fundamental contribution of our work consists in the fact that we unveiled two complementary connectivity mechanisms (i.e. both amplitude and phase synchronization), measured respectively by spectral and imaginary coherence, that occurred simultaneously during the MI task. Then, we demonstrated the contribution of brain network connectivity features in detecting mental states during typical MI-based BCI tasks. Taken together, our results provide fresh insights into the network mechanisms subserving brain functional changes during MI, and offer new perspectives to improve BCI performance.

Acknowledgment

The authors would like to acknowledge Mario Chavez for useful discussion and suggestions. The content is solely the responsibility of the authors and does not necessarily represent the official views of any of the funding agencies.

References

[1] C. Vidaurre and B. Blankertz, "Towards a cure for BCI illiteracy," *Brain Topograp.*, vol. 23, no. 2, pp. 194–198, Jun. 2010.
[2] M. C. Thompson, "Critiquing the concept of BCI illiteracy," *Sci. Eng. Ethics*, vol. 25, no. 4, pp. 1217–1233, Aug. 2019.
[3] T. Carlson and J. del R. Millan, "Brain-controlled wheelchairs: A robotic architecture," *IEEE Robot. Autom. Mag.*, vol. 20, no. 1, pp. 65–73, Mar. 2013.
[4] B. Z. Allison and C. Neuper, "Could anyone use a BCI?" in *Brain-Computer Interfaces*. London, U.K.: Springer, 2010, pp. 35–54.
[5] T. Dickhaus *et al.*, "Predicting BCI performance to study BCI illiteracy," *BMC Neurosci.*, vol. 10, p. P84, 2009, doi: 10.1186/1471-2202-10-S1-P84.

[6] G. Edlinger, B. Z. Allison, and C. Guger, "How many people can use a BCI system?" in *Clinical Systems Neuroscience*, K. Kansaku, L. Cohen, and N. Birbaumer, Eds. Tokyo, Japan: Springer, 2015, doi: 10.1007/978-4-431-55037-2_3.

[7] M. Ahn and S. C. Jun, "Performance variation in motor imagery brain–computer interface: A brief review," *J. Neurosci. Methods*, vol. 243, pp. 103–110, Mar. 2015.

[8] G. Muller-Putz *et al.*, "Towards noninvasive hybrid brain–computer interfaces: Framework, practice, clinical application, and beyond," *Proc. IEEE*, vol. 103, no. 6, pp. 926–943, Jun. 2015.

[9] C. Vidaurre, C. Sannelli, K.-R. Müller, and B. Blankertz, "Co-adaptive calibration to improve BCI efficiency," *J. Neural Eng.*, vol. 8, no. 2, Apr. 2011, Art. no. 025009.

[10] F. Lotte, M. Congedo, A. Lécuyer, F. Lamarche, and B. Arnaldi, "A review of classification algorithms for eeg-based brain–computer interfaces," *J. Neural Eng.*, vol. 4, no. 2, p. R1, 2007.

[11] A. E. van Delden *et al.*, "Comparing unilateral and bilateral upper limb training: The ULTRA-stroke program design," *BMC Neurol.*, vol. 9, no. 1, p. 57, Dec. 2009.

[12] F. De Vico Fallani, J. Richiardi, M. Chavez, and S. Achard, "Graph analysis of functional brain networks: Practical issues in translational neuroscience," *Phil. Trans. Roy. Soc. B, Biol. Sci.*, vol. 369, no. 1653, Oct. 2014, Art. no. 20130521.

[13] F. De Vico Fallani and D. S. Bassett, "Network neuroscience for optimizing brain–computer interfaces," *Phys. Life Rev.*, vol. 31, pp. 304–309, Dec. 2019.

[14] R. Zhang *et al.*, "Efficient resting-state EEG network facilitates motor imagery performance," *J. Neural Eng.*, vol. 12, no. 6, Dec. 2015, Art. no. 066024.

[15] T. Zhang *et al.*, "Structural and functional correlates of motor imagery BCI performance: Insights from the patterns of fronto-parietal attention network," *NeuroImage*, vol. 134, pp. 475–485, Jul. 2016.

[16] F. Li *et al.*, "The dynamic brain networks of motor imagery: Time-varying causality analysis of scalp EEG," *Int. J. Neural Syst.*, vol. 29, no. 1, Feb. 2019, Art. no. 1850016.

[17] M. Hamedi, S.-H. Salleh, and A. M. Noor, "Electroencephalographic motor imagery brain connectivity analysis for BCI: A review," *Neural Comput.*, vol. 28, no. 6, pp. 999–1041, Jun. 2016.

[18] Q. Wei, Y. Wang, X. Gao, and S. Gao, "Amplitude and phase coupling measures for feature extraction in an eeg-based brain–computer interface," *J. Neural Eng.*, vol. 4, no. 2, p. 120, 2007.

[19] L. Song, E. Gordon, and E. Gysels, "Phase synchrony rate for the recognition of motor imagery in brain–computer interface," in *Proc. Adv. Neural Inf. Process. Syst.*, 2006, pp. 1265–1272.

[20] C. Brunner, B. Graimann, J. E. Huggins, S. P. Levine, and G. Pfurtscheller, "Phase relationships between different subdural electrode recordings in man," *Neurosci. Lett.*, vol. 375, no. 2, pp. 69–74, Feb. 2005.

[21] G. C. Carter, "Coherence and time delay estimation," *Proc. IEEE*, vol. 75, no. 2, pp. 236–255, Feb. 1987.

[22] G. Nolte, O. Bai, L. Wheaton, Z. Mari, S. Vorbach, and M. Hallett, "Identifying true brain interaction from EEG data using the imaginary part of coherency," *Clin. Neurophysiol.*, vol. 115, no. 10, pp. 2292–2307, Oct. 2004.

[23] M. G. Rosenblum, A. S. Pikovsky, and J. Kurths, "Phase synchronization of chaotic oscillators," *Phys. Rev. Lett.*, vol. 76, no. 11, p. 1804, Mar. 1996.

[24] J. R. Wolpaw, D. J. McFarland, T. M. Vaughan, and G. Schalk, "The wadsworth center brain-computer interface (BCI) research and development program," *IEEE Trans. Neural Syst. Rehabil. Eng.*, vol. 11, no. 2, pp. 1–4, Jun. 2003.

[25] M.-C. Corsi *et al.*, "Integrating EEG and MEG signals to improve motor imagery classification in brain–computer interface," *Int. J. Neural Syst.*, vol. 29, no. 1, Feb. 2019, Art. no. 1850014.

[26] A. J. Bell and T. J. Sejnowski, "An information-maximization approach to blind separation and blind deconvolution," *Neural Comput.*, vol. 7, no. 6, pp. 1129–1159, Nov. 1995.

[27] R. Oostenveld, P. Fries, E. Maris, and J.-M. Schoffelen, "FieldTrip: Open source software for advanced analysis of MEG, EEG, and invasive electrophysiological data," *Comput. Intell. Neurosci.*, vol. 2011, pp. 1–9, 2011.

[28] B. Blankertz, G. Dornhege, M. Krauledat, K.-R. Müller, and G. Curio, "The non-invasive Berlin brain–computer interface: Fast acquisition of effective performance in untrained subjects," *NeuroImage*, vol. 37, no. 2, pp. 539–550, Aug. 2007.

[29] A. M. Bastos and J.-M. Schoffelen, "A tutorial review of functional connectivity analysis methods and their interpretational pitfalls," *Frontiers Syst. Neurosci.*, vol. 9, p. 175, Jan. 2016.

[30] E. Gysels and P. Celka, "Phase synchronization for the recognition of mental tasks in a brain-computer interface," *IEEE Trans. Neural Syst. Rehabil. Eng.*, vol. 12, no. 4, pp. 406–415, Dec. 2004.

[31] F. Pichiorri *et al.*, "Brain-computer interface boosts motor imagery practice during stroke recovery," *Ann. Neurol.*, vol. 77, no. 5, pp. 851–865, May 2015.

[32] M. Grosse-Wentrup, "Understanding brain connectivity patterns during motor imagery for brain-computer interfacing," in *Proc. Adv. Neural Inf. Process. Syst.*, 2009, pp. 561–568.

[33] D. J. Krusienski, D. J. McFarland, and J. R. Wolpaw, "Value of amplitude, phase, and coherence features for a sensorimotor rhythm-based brain–computer interface," *Brain Res. Bull.*, vol. 87, no. 1, pp. 130–134, Jan. 2012.

[34] P. Welch, "The use of fast Fourier transform for the estimation of power spectra: A method based on time averaging over short, modified periodograms," *IEEE Trans. Audio Electroacoust.*, vol. AE-15, no. 2, pp. 70–73, Jun. 1967.

[35] T. Cattai, S. Colonnese, M.-C. Corsi, D. S. Bassett, G. Scarano, and F. De Vico Fallani, "Characterization of mental states through node connectivity between brain signals," in *Proc. 26th Eur. Signal Process. Conf. (EUSIPCO)*, Sep. 2018, pp. 1391–1395.

[36] G. Pfurtscheller and C. Neuper, "Future prospects of ERD/ERS in the context of brain-computer interface (BCI) developments," in *Event-Related Dynamics of Brain Oscillations* (Progress in Brain Research), vol. 159, C. Neuper and W. Klimesch, Eds. Amsterdam, The Netherlands: Elsevier, 2006, pp. 433–437. [Online]. Available: https://www.sciencedirect.com/science/article/pii/S0079612306590284

[37] J. H. Zar, *Biostatistical Analysis*. New Delhi, India: Pearson Education, 1999.

[38] C. Neuper and G. Pfurtscheller, "Event-related dynamics of cortical rhythms: Frequency-specific features and functional correlates," *Int. J. Psychophysiol.*, vol. 43, no. 1, pp. 41–58, Dec. 2001.

[39] G. Pfurtscheller, "Spatiotemporal ERD/ERS patterns during voluntary movement and motor imagery," in *Supplements to Clinical Neurophysiology*, vol. 53. Amsterdam, The Netherlands: Elsevier, 2000, pp. 196–198.

[40] F. Ferri, P. Pudil, M. Hatef, and J. Kittler, "Comparative study of techniques for large-scale feature selection," in *Machine Intelligence and Pattern Recognition*, vol. 16. Amsterdam, The Netherlands: Elsevier, 1994, pp. 403–413.

[41] Y. Benjamini and Y. Hochberg, "Controlling the false discovery rate: A practical and powerful approach to multiple testing," *J. Roy. Stat. Soc. Ser. B, Methodol.*, vol. 57, no. 1, pp. 289–300, Jan. 1995.

[42] K. K. Ang, Z. Y. Chin, C. Wang, C. Guan, and H. Zhang, "Filter bank common spatial pattern algorithm on BCI competition IV datasets 2a and 2b," *Frontiers Neurosci.*, vol. 6, no. 1, p. 39, 2012.

[43] G. Pfurtscheller, "EEG event-related desynchronization (ERD) and synchronization (ERS)," *Electroencephalogr. Clin. Neurophysiol.*, vol. 103, no. 1, p. 26, Jul. 1997.

[44] G. Pfurtscheller and F. H. Lopes da Silva, "Event-related EEG/MEG synchronization and desynchronization: Basic principles," *Clin. Neurophysiol.*, vol. 110, no. 11, pp. 1842–1857, Nov. 1999.

[45] V. N. Murthy and E. E. Fetz, "Coherent 25-to 35-Hz oscillations in the sensorimotor cortex of awake behaving monkeys," *Proc. Nat. Acad. Sci. USA*, vol. 89, no. 12, p. 5670, 1992.

[46] T. Jiang, Y. He, Y. Zang, and X. Weng, "Modulation of functional connectivity during the resting state and the motor task," *Hum. Brain Mapping*, vol. 22, no. 1, pp. 63–71, 2004.

[47] Y. Meirovitch, H. Harris, E. Dayan, A. Arieli, and T. Flash, "Alpha and beta band event-related desynchronization reflects kinematic regularities," *J. Neurosci.*, vol. 35, no. 4, pp. 1627–1637, Jan. 2015.

[48] M. Denker *et al.*, "LFP beta amplitude is linked to mesoscopic spatio-temporal phase patterns," *Sci. Rep.*, vol. 8, no. 1, p. 5200, Dec. 2018.

[49] N. E. Crone, A. Sinai, and A. Korzeniewska, "High-frequency gamma oscillations and human brain mapping with electrocorticography," *Prog. brain Res.*, vol. 159, pp. 275–295, Jan. 2006.

[50] J. Hipp, D. Hawellek, M. Corbetta, M. Siegel, and A. Engel, "Large-scale cortical correlation structure of spontaneous oscillatory activity," *Nature Neurosci.*, vol. 15, pp. 884–890, May 2012.

[51] I. Daly, S. J. Nasuto, and K. Warwick, "Brain computer interface control via functional connectivity dynamics," *Pattern Recognit.*, vol. 45, no. 6, pp. 2123–2136, Jun. 2012.

[52] F. De Vico Fallani *et al.*, "Evaluation of the brain network organization from EEG signals: A preliminary evidence in stroke patient," *Anatomical Rec. Adv. Integrative Anatomy Evol. Biol.*, vol. 292, no. 12, pp. 2023–2031, Dec. 2009.

[53] M.-E. Lynall *et al.*, "Functional connectivity and brain networks in schizophrenia," *J. Neurosci.*, vol. 30, no. 28, pp. 9477–9487, 2010.

[54] B. C. M. van Wijk, P. J. Beek, and A. Daffertshofer, "Neural synchrony within the motor system: What have we learned so far?" *Frontiers Hum. Neurosci.*, vol. 6, p. 252, Sep. 2012.

[55] C. Neuper and W. Klimesch, *Event-Related Dynamics of Brain Oscillations*, vol. 159. Amsterdam, The Netherlands: Elsevier, 2006.

[56] Q. Qiu *et al.*, "Origin of amplitude synchronization in coupled nonidentical oscillators," *Phys. Rev. E, Stat. Phys. Plasmas Fluids Relat. Interdiscip. Top.*, vol. 101, no. 2, Feb. 2020, Art. no. 022210. [Online]. Available: https://link.aps.org/doi/10.1103/PhysRevE.101.022210

[57] M. Siems and M. Siegel, "Dissociated neuronal phase- and amplitude-coupling patterns in the human brain," *NeuroImage*, vol. 209, Apr. 2020, Art. no. 116538. [Online]. Available: https://www.sciencedirect.com/science/article/pii/S1053811920300252

[58] Y. Li *et al.*, "Global synchronization in the theta band during mental imagery of navigation in humans," *Neurosci. Res.*, vol. 65, no. 1, pp. 44–52, Sep. 2009, doi: 10.1016/j.neures.2009.05.004.

[59] S. Hori *et al.*, "Alpha- and theta-range cortical synchronization and corticomuscular coherence during joystick manipulation in a virtual navigation task," *Brain Topograp.*, vol. 26, pp. 591–605, Jun. 2013.

[60] K.-R. Müller, M. Tangermann, G. Dornhege, M. Krauledat, G. Curio, and B. Blankertz, "Machine learning for real-time single-trial EEG-analysis: From brain–computer interfacing to mental state monitoring," *J. Neurosci. Methods*, vol. 167, no. 1, pp. 82–90, Jan. 2008.

[61] A. Barachant, S. Bonnet, M. Congedo, and C. Jutten, "Riemannian geometry applied to BCI classification," in *Latent Variable Analysis and Signal Separation* (Lecture Notes in Computer Science), vol. 6365, V. Vigneron, V. Zarzoso, E. Moreau, R. Gribonval, and E. Vincent, Eds. Berlin, Germany: Springer, 2010, doi: 10.1007/978-3-642-15995-4_78.

[62] P. Gaur, R. B. Pachori, H. Wang, and G. Prasad, "A multi-class eeg-based BCI classification using multivariate empirical mode decomposition based filtering and Riemannian geometry," *Expert Syst. Appl.*, vol. 95, pp. 201–211, Apr. 2018.

[63] D. L. Rocca *et al.*, "Human brain distinctiveness based on EEG spectral coherence connectivity," *IEEE Trans. Biomed. Eng.*, vol. 61, no. 9, pp. 2406–2412, Sep. 2014.

[64] M. Hamedi, S.-H. Salleh, S. B. Samdin, and A. M. Noor, "Motor imagery brain functional connectivity analysis via coherence," in *Proc. IEEE Int. Conf. Signal Image Process. Appl. (ICSIPA)*, Oct. 2015, pp. 269–273.

[65] C. Brunner, R. Scherer, B. Graimann, G. Supp, and G. Pfurtscheller, "Online control of a brain-computer interface using phase synchronization," *IEEE Trans. Biomed. Eng.*, vol. 53, no. 12, pp. 2501–2506, Dec. 2006.

[66] N. Caramia, F. Lotte, and S. Ramat, "Optimizing spatial filter pairs for EEG classification based on phase-synchronization," in *Proc. IEEE Int. Conf. Acoust., Speech Signal Process. (ICASSP)*, May 2014, pp. 2049–2053.

[67] C. Gouy-Pailler *et al.*, "Topographical dynamics of brain connections for the design of asynchronous brain-computer interfaces," in *Proc. 29th Annu. Int. Conf. IEEE Eng. Med. Biol. Soc.*, Aug. 2007, pp. 2520–2523.

[68] R. Salazar-Varas and D. Gutiérrez, "Feature extraction for multi-class BCI using EEG coherence," in *Proc. 7th Int. IEEE/EMBS Conf. Neural Eng. (NER)*, Apr. 2015, pp. 94–97.

[69] A. Y. Kaplan, A. A. Fingelkurts, A. A. Fingelkurts, S. V. Borisov, and B. S. Darkhovsky, "Nonstationary nature of the brain activity as revealed by EEG/MEG: Methodological, practical and conceptual challenges," *Signal Process.*, vol. 85, no. 11, pp. 2190–2212, Nov. 2005.

[70] D. Kwiatkowski, P. C. B. Phillips, P. Schmidt, and Y. Shin, "Testing the null hypothesis of stationarity against the alternative of a unit root: How sure are we that economic time series have a unit root?" *J. Econometrics*, vol. 54, nos. 1–3, pp. 159–178, 1992.

[71] M. Le Van Quyen *et al.*, "Comparison of Hilbert transform and wavelet methods for the analysis of neuronal synchrony," *J. Neurosci. Methods*, vol. 111, no. 2, pp. 83–98, Sep. 2001.

[72] A. Ozdemir, E. M. Bernat, and S. Aviyente, "Recursive tensor subspace tracking for dynamic brain network analysis," *IEEE Trans. Signal Inf. Process. Over Netw.*, vol. 3, no. 4, pp. 669–682, Dec. 2017.

[73] R. D. Pascual-Marqui, "Coherence and phase synchronization: Generalization to pairs of multivariate time series, and removal of zero-lag contributions," 2007, *arXiv:0706.1776*. [Online]. Available: http://arxiv.org/abs/0706.1776

[74] M. A. Jatoi, N. Kamel, A. S. Malik, I. Faye, and T. Begum, "A survey of methods used for source localization using EEG signals," *Biomed. Signal Process. Control*, vol. 11, pp. 42–52, May 2014.

[75] C. M. Michel, M. M. Murray, G. Lantz, S. Gonzalez, L. Spinelli, and R. G. de Peralta, "EEG source imaging," *Clin. Neurophysiol.*, vol. 115, no. 10, pp. 2195–2222, Oct. 2004.

[76] B. J. Edelman, B. Baxter, and B. He, "EEG source imaging enhances the decoding of complex right-hand motor imagery tasks," *IEEE Trans. Biomed. Eng.*, vol. 63, no. 1, pp. 4–14, Jan. 2016.

[77] S. Baillet, J. C. Mosher, and R. M. Leahy, "Electromagnetic brain mapping," *IEEE Signal Process. Mag.*, vol. 18, no. 6, pp. 14–30, Nov. 2001.

[78] K. Mahjoory, V. V. Nikulin, L. Botrel, K. Linkenkaer-Hansen, M. M. Fato, and S. Haufe, "Consistency of EEG source localization and connectivity estimates," *NeuroImage*, vol. 152, pp. 590–601, May 2017.

[79] D. Ruta and B. Gabrys, "An overview of classifier fusion methods," *Comput. Inf. Syst.*, vol. 7, no. 1, pp. 1–10, 2000.